Charge Movement by the Na/K Pump
in *Xenopus* Oocytes

R. F. RAKOWSKI

From the Department of Physiology and Biophysics, University of Health Sciences/The Chicago Medical School, North Chicago, Illinois 60064

ABSTRACT   Pre–steady-state transient currents (1986. Nakao, M., and D. C. Gadsby. *Nature [Lond.]*. 323:628–630) mediated by the Na/K pump were measured under conditions for Na/Na exchange (K-free solution) in voltage-clamped *Xenopus* oocytes. Signal-averaged (eight times) current records obtained in response to voltage clamp steps over the range −160 to +60 mV after the addition of 100 μM dihydroouabain (DHO) or removal of external Na (control) were subtracted from test records obtained before the solution change. A slow component of DHO- or Na-sensitive difference current was consistently observed and its properties were analyzed. The quantity of charge moved was well described as a Boltzmann function of membrane potential with an apparent valence of 1.0. The relaxation rate of the current was fit by the sum of an exponentially voltage-dependent reverse rate coefficient plus a voltage-independent forward rate constant. The quantity of charge moved at the on and off of each voltage pulse was approximately equal except at extreme negative values of membrane potential where the on charge tended to be less than the off. The midpoint voltage of the charge distribution function (V_q) was shifted by −24.8 ± 1.7 mV by changing the external [Na] in the test condition from 90 to 45 mM and by +14.7 ± 1.7 mV by changing the test [Na] from 90 to 120 mM. A pseudo three-state model of charge translocation is discussed in which Na^+ is bound and occluded at the internal face of the enzyme and is released into an external-facing high field access channel (ion well). The model predicts a shift of the charge distribution function to more hyperpolarized potentials as extracellular [Na] is lowered; however, several features of the data are not predicted by the model.

INTRODUCTION

Pre–Steady-State Transient Current Mediated by the Na/K Pump

Nakao and Gadsby (1986) were the first to record pre–steady-state transient current mediated by the Na/K pump in response to imposed voltage steps. Isolated guinea pig ventricular myocytes were voltage clamped and internally dialyzed with wide-tipped pipettes. Under K-free conditions, strophanthidin-sensitive transient currents were recorded that could be attributed to charge translocation under electroneutral Na/Na exchange conditions. The voltage dependence of the quantity of charge

Address reprint requests to Dr. R. F. Rakowski, Department of Physiology and Biophysics, University of Health Sciences/The Chicago Medical School, 3333 Green Bay Road, North Chicago, IL 60064.

moved could be described by a saturating sigmoid relationship derived from the Boltzmann equation with an exponential steepness factor of 26.5 mV, appropriate for the movement of one net charge through the entire membrane field. The transient currents declined monoexponentially to zero as expected for a net electroneutral Na/Na exchange process. The rate coefficients of the charge relaxation were found to be asymmetrically voltage dependent, with almost all of the voltage-dependent increase with hyperpolarization falling on the reverse rate coefficient and little or no voltage dependence falling on the forward rate coefficient (De Weer, 1990). Subsequent work by Bahinski, Nakao, and Gadsby (1988) has established that as external [K] is increased in the bathing solution, the steady-state Na/K pump current increases and is accompanied by a decrease in the magnitude of the pre–steady-state transient current. These authors were unable to measure strophanthidin-sensitive pre–steady-state charge movement under conditions of K/K exchange, leading them to conclude that K translocation is voltage insensitive. This conclusion, however, is overly broad since the charge movement data were obtained at saturating external [K], and it has subsequently been established that the existence of a second voltage-dependent step (in the K translocation pathway) is required to explain the occurrence of a negative slope in the forward Na/K pump current–voltage (I-V) relationship when external [K] is reduced below saturation (Rakowski, Vasilets, LaTona, and Schwarz, 1991). Transient Na/K pump currents have also been observed by flash photolysis of caged ATP (Fendler, Grell, Haubs, and Bamberg, 1985; Borlinghaus, Apell, and Läuger, 1987).

Voltage Dependence of Na Efflux Mediated by Electroneutral Na/Na Exchange

A major clarification and simplification of our understanding of the nature of the voltage-dependent steps in the Na half-cycle of the Na/K pump has been achieved by recent investigations of the steady-state voltage dependence of ^{22}Na efflux mediated by electroneutral Na/Na exchange (Gadsby, D. C., R. F. Rakowski, and P. De Weer, manuscript submitted for publication). The simple fact that Na efflux saturates at hyperpolarized potentials rather than following a bell-shaped curve leads to the conclusion that under these experimental conditions only the rate coefficients in the Na half-cycle associated with external Na binding are voltage dependent and that Na release is voltage independent (De Weer, Rakowski, and Gadsby, 1992). This asymmetrical effect is easiest to explain if the binding rate depends on Na entry into an external high-field access channel (ion well) in the pump molecule. This hypothesis has several testable predictions, the strongest of which is that changes in external [Na] and voltage should be kinetically equivalent, so that the midpoint voltage of the relationships used to describe charge movement and the forward and reverse Na/K pump I-V relationships should be shifted along the voltage axis by changes in external [Na] (see Appendix).

The experiments described in this paper were designed to confirm and extend the characterization of Na/K pump–mediated pre–steady-state charge movement and to test the prediction of shifts in its voltage dependence by changes in external [Na].

A preliminary report of these findings has been published (Rakowski, 1992).

METHODS

Preparation of Oocytes

Commercially bred and reared, oocyte-positive, adult female African clawed toads (*Xenopus laevis*) were maintained on a high protein diet in fresh water tanks and were killed by decapitation after being anesthetized by immersion in crushed ice. Pieces of the ovary were removed and the oocytes were dissociated by treatment for 1–2 h with collagenase (0.6–0.8 U/ml) in oocyte Ringer's solution (Rakowski et al., 1991). Intracellular [Na] was elevated either by incubation for 2 h at room temperature in Ca- and K-free Na citrate loading solution (LaTona, 1990; Rakowski et al., 1991) or by overnight incubation at 16–17°C in K-free oocyte Ringer's solution.

Solutions

The normal 90 mM Na (test) solution had the following composition (mM): 90 NaCl, 5 BaCl$_2$, 20 tetraethylammonium (TEA) chloride, 2 NiCl$_2$, 5 MOPS (pH 7.6). Na-free (control) solution was prepared by substitution of N-methyl D-glucamine (NMG) chloride for NaCl, and 45 mM Na solution was made by mixing equal parts of 90 mM Na and Na-free solution. Hypertonic 120 mM Na solution was prepared by using 120 mM rather than 90 mM NaCl. Results in this solution were compared with experiments in a 90 mM Na solution made hypertonic by addition of 30 mM NMG chloride. The various solutions are hereafter referred to as 90 Na, Na-free, 45 Na, 120 Na, and hypertonic 90 Na. The solutions were designed to minimize non–pump-mediated currents. TEA and Ba^{2+} were present to reduce K channel–mediated resting and time-dependent currents. Note also that all solutions are K free, in order to prevent the normal forward mode of Na/K pump operation and promote electroneutral Na/Na exchange. All solutions were also Ca free to prevent outward Na/Ca exchange current and contained 2 mM Ni^{2+} to block any possible inward Na/Ca exchange current. This concentration of Ni^{2+} has been shown to have little or no effect on forward Na$^+$/K$^+$ pumping in oocytes (Rakowski et al., 1991). It is not known whether there is an effect of either Ba^{2+} or Ni^{2+} on the pre–steady-state transients described here.

Electrophysiological Measurements

A high output compliance (±120 V) two-microelectrode voltage clamp system (model OC725; Warner Instruments, Hamden, CT) was used to maintain the holding potential and to apply command voltage pulses. Before data collection the clamp gain was adjusted to obtain optimally square step responses to 20-mV depolarizing pulses. The intracellular current electrodes were filled with 2 M K citrate, were shielded with Al foil, and had resistances of 0.5–2 MΩ. Intracellular voltage recording electrodes were filled with 3 M KCl and had resistances of 1–5 MΩ. The bath electrodes were low resistance agar bridges that were connected to 3 M KCl-filled pools equipped with Ag/AgCl$_2$ electrodes at the solution/metal interface. Extra care was taken to minimize lead lengths and electrode impedances in order to obtain low noise recordings and relatively rapid step responses despite the large capacitance of the oocyte membrane.

Data were collected using a commercially available analog to digital (A-D) converter system (TL-1 DMA interface, 100 kHz; Axon Instruments, Inc., Foster City, CA) and software (PCLAMP version 5.5; Axon Instruments, Inc.) running on an IBM compatible computer system (model 210; Dell Computer Corp., Austin, TX). The data were filtered at 1 kHz, sampled at 200 μs per point, and signal-averaged eight times before and after each solution change. Subtraction of current records and the least-squares data analysis to determine the exponential relaxation rate (k_s) and the initial magnitude of the slow component of difference

current ($I_s(0)$) were performed with the CLAMPFIT software module of PCLAMP. Further analysis, least-squares curve fitting, and preparation of figures was done with SIGMAPLOT software (version 4.0; Jandel Scientific, Corte Madera, CA). The error limits given for parameters obtained by least-squares curve fitting represent ±1 SD. Experiments were performed at room temperature (22°C).

RESULTS

Transient and Steady-State Current Records Measured in 90 Na and Na-free Solution

It is quite remarkable that the difference in the time course of membrane current recorded in 90 Na and Na-free solutions can be seen directly before subtraction. Direct visual comparison of the signal-averaged current records in 90 Na (Fig. 1 B) and Na-free solution (Fig. 1 C) clearly shows that after the initial capacitive current transient (off scale at this gain) the current declines more slowly to its steady-state value in 90 Na than in Na-free solution. The difference is even more apparent on comparison of the tail current records upon returning to the holding potential (−40 mV). Fig. 1 D shows that Na removal has essentially no effect on the steady-state current–voltage (I-V) relationship, indicating that there is little or no steady-state Na-dependent current under these K- and Ca-free conditions.

Capacitive Current Time Course

Before proceeding to analyze the Na-sensitive difference current that may be calculated from the records shown in Fig. 1, it is appropriate to determine what the time course of the linear capacitive current transient is, and thereby determine the temporal resolution of the recording system. As shown in Fig. 2 B, at the high current gain used for these experiments, the capacitive current transients recorded at the off of the records in Fig. 1 C produce saturation of the A-D converter system even for the smallest (20 mV) excursions from the resting potential. Recovery from overload is rapid, however, and only occasionally does a single subsequent data point on a given record deviate from the single exponential decay rate expected for 1-kHz filtered data. Even for the largest voltage steps, current subtraction should be reproducible and accurate after ~1.5 ms, the longest duration of the period of saturation. The linear component of capacitive current declines to the level of the noise within ~4 ms after a voltage step.

Reproducibility of Current Subtraction

A direct demonstration of the reproducibility of current subtraction is shown in Fig. 2 C. The difference current was calculated by subtraction of the records in Fig. 1 B from current records obtained in the same oocyte 5 min beforehand under identical experimental conditions. The current records are reproducible to within a peak-to-peak current noise of ~5–10 nA even during the capacitive current transient and the period of A-D converter saturation at the on and off of the current record. This high degree of reproducibility at the on and off is achievable, in part, as a result of both the command pulse and A-D converter timing being controlled by the same crystal clock. The reproducibility of the steady-state level of current at the end of the voltage
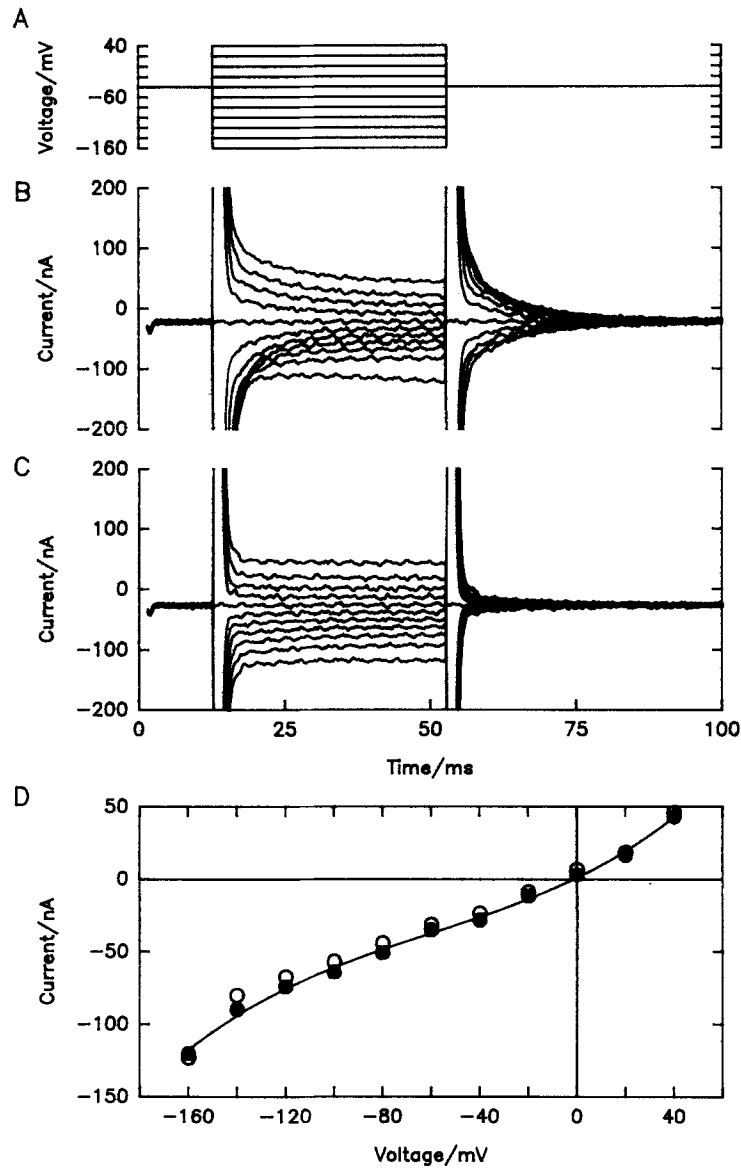
FIGURE 1. Time course of membrane current in 90 Na and Na-free solutions. (*A*) Voltage pulse protocol. Holding potential = −40 mV. (*B*) Current time course in 90 mM Na, K-free solution, signal-averaged eight times in response to the pulse protocol in *A*. (*C*) Current time course in Na-free and K-free solution, signal-averaged eight times, 5 min after changing from 90 Na. (*D*) Steady-state *I-V* relationship measured at the end of each voltage pulse in *B* and *C*. *Filled symbols*, 90 mM Na; *open symbols*, Na-free solution. Temperature, 22°C.
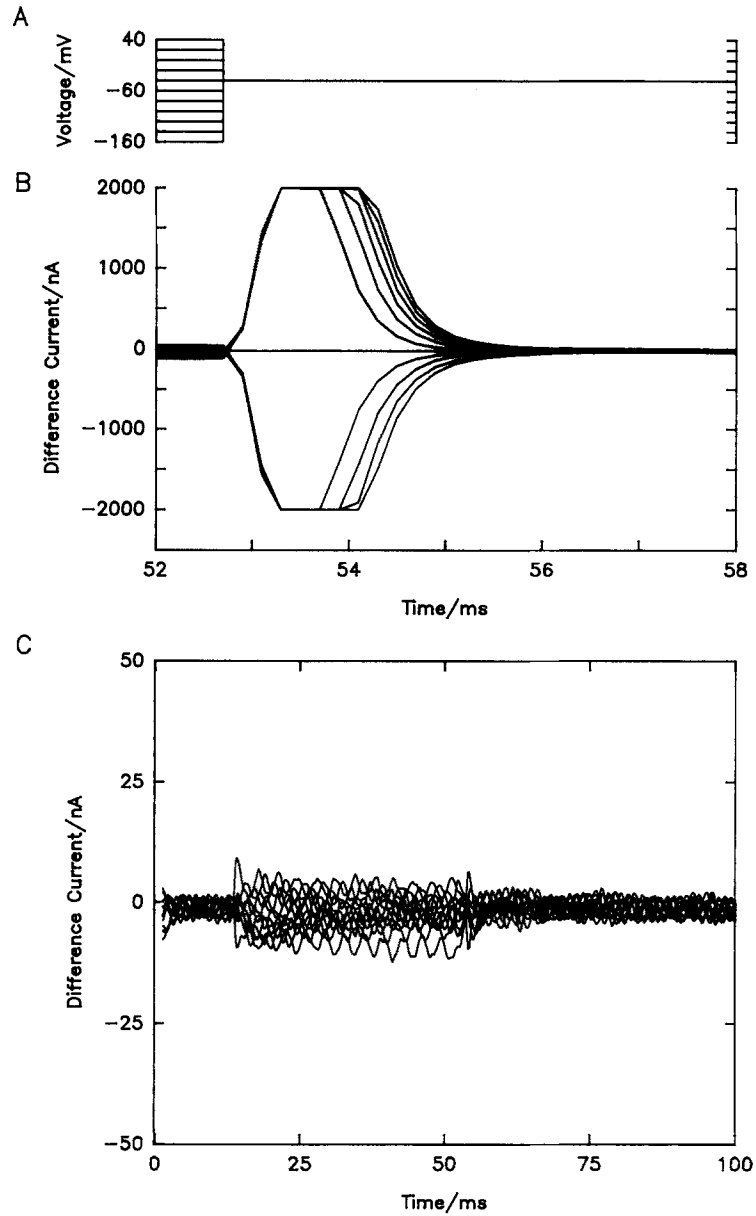
FIGURE 2. Capacity current time course and reproducibility of the subtraction of membrane current. (A) Voltage pulse protocol at the off of the data shown in Fig. 1 C. (B) Capacity current time course upon returning to the holding potential of −40 mV. The analog to digital converter system saturates at ± 2,000 nA. Note the greatly expanded time scale. (C) Difference current record obtained by subtraction of the current records in Fig. 1 B from records obtained in the same oocyte 5 min previously under identical experimental conditions. Voltage pulse protocol as in Fig. 1 A.

pulse provides a convenient check for the D.C. stability of the recording electrodes and resting conductance of the oocyte.
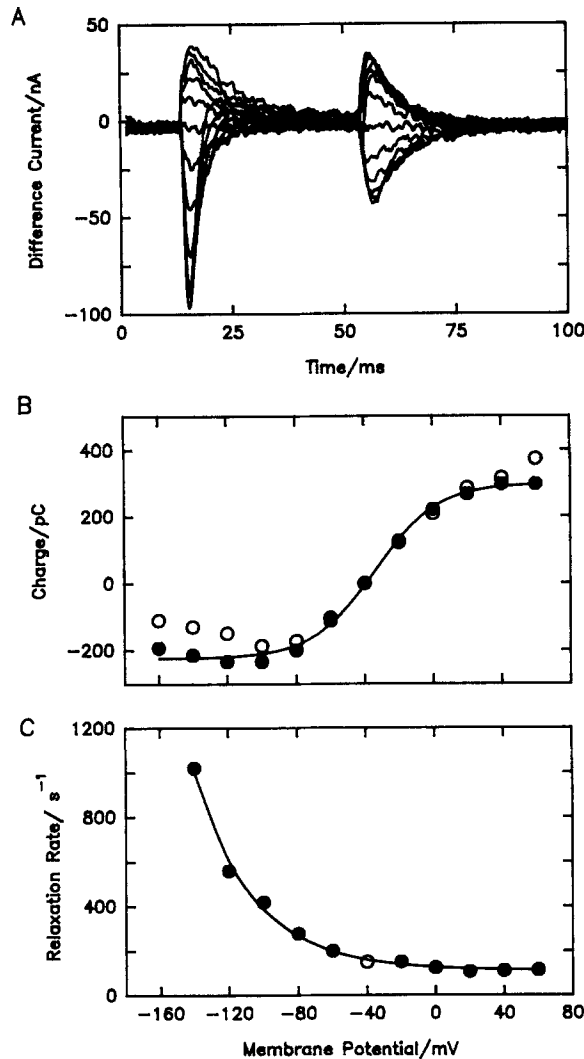

FIGURE 3. Characteristics of the slow component of Na-sensitive current (I_s). (A) Na-sensitive difference current measured in an oocyte by subtraction of current records before and after the third solution change from 90 Na to Na-free solution. (B) Voltage dependence of the slow component of Na-sensitive charge (Q_s). *Filled symbols*, charge calculated from the off tail currents in A according to the relationship $Q_s = I_s(0)/k_s$. *Open symbols*, charge calculated in a similar way from the on transient current. The solid line is at least-squares fit of the solid symbols by Eq. 2. The best-fit parameters are $Q_{smin} = -224 \pm 9$ pC, $Q_{stot} = 523 \pm 17$ pC, $z_q = 1.38 \pm 0.14$, and $V_q = -33.7 \pm 2.1$ mV. (C) Voltage dependence of the relaxation rates (k_s) was determined by fitting a single exponential decay equation to the data of the form $I_s = I_s(0) \exp(-k_s t)$, where t is the time after the voltage step and $I_s(0)$ is the magnitude of I_s extrapolated back to the time of the step. The data were fit during the time from 4 to 6 ms after the voltage step until the end of the pulse. *Filled symbols*, k_s determined from the data during each voltage pulse. *Open symbol*, k_s determined from the tail currents at the off of the pulse. The SEM is smaller than the symbol radius. The solid line is at least-squares fit of the data by Eq. 1. The best-fit parameter values are: $a_k = 112 \pm 11$ s^{-1}, $z_k = 0.743 \pm 0.044$, and $V_k = -69 \pm 7$ mV.

Na-sensitive Difference Currents

A typical result of the subtraction of control current records in Na-free solution from test records in 90 Na is shown in Fig. 3 A. In several cases, in addition to the current shown in Fig. 3 A, a large, fast component of difference current that occurs within the

duration of the linear capacitive current was observed. However, this fast transient current was not seen in subsequent records from the same oocyte, and was therefore not analyzed in detail. A fast transient component of charge movement is expected to occur as redistribution of ions takes place within the postulated access channel. Hilgemann, Philipson, and Nicoll (1992) have reported a fast charge movement possibly associated with extracellular Na binding by the Na/K pump in cardiac myocytes voltage clamped using the giant excised patch technique. Further studies of these fast current transients may be of considerable interest, but will require better temporal resolution than can be achieved with the two-microelectrode technique.

Characteristics of the Slow Component of Na-sensitive Charge (Q_s)

Results of the analysis of the Na-sensitive difference current records in Fig. 3 A are shown in Fig. 3, B and C. The relaxation rates (k_s) were obtained by a least-squares exponential fit to the data from 4–6 ms after each voltage step until the end of that step. An estimate of the initial magnitude of the slow component of current ($I_s(0)$) was obtained by back-extrapolation of the least-squares curve fit to the start of each voltage step. The relaxation rates are well described as the sum of a forward voltage-independent rate constant (a_k) and a reverse voltage-dependent rate coefficient according to Eq. 1, which may be derived from Eq. A2 in the Appendix:

$$k_s = a_k\{1 + \exp[z_k(V_k - V)F/RT]\} \tag{1}$$

The magnitudes of the slow component of on (Q_s(on)) and off (Q_s(off)) charge were calculated according to $Q_s = I_s(0)/k_s$ and are plotted in Fig. 3 B. The values of Q_s(on) (open symbols) tend to be less than the values of Q_s(off) at hyperpolarized voltages. The values of Q_s(off) (filled symbols) have been fitted by Eq. 2, which may be derived from Eq. A7 or A21 in the Appendix:

$$Q_s = Q_{smin} + \langle Q_{stot}\{1 + \exp[z_q(V_q - V)F/RT]\}\rangle \tag{2}$$

The best-fit parameters for this oocyte are given in the figure legend. Although Eqs. 1 and 2 have been derived for two specific models as discussed in the Appendix, it should be clear that these equations represent canonical forms that are characteristic of a large class of models in which there are one or more exponentially voltage-dependent steps. The various parameters in these two equations are relatively model independent and can be uniquely determined by a least-squares fit to the data. They are, therefore, adopted as a convenient means of characterizing the data. As discussed in the Appendix, it is possible to derive the specific relationship between, for example, the midpoint voltage V_q and the individual rate constants of a particular kinetic model (cf. Eqs. A8 and A22 in the Appendix). Unfortunately, these measurements do not provide sufficient information to uniquely determine the individual rate constants of any but the simplest kinetic model. That being the case, only the parameters of Eqs. 1 and 2 that are uniquely determinable will be given in the Results. An attempt to determine individual rate constants for a particular model by simultaneously fitting both the Q vs. V and relaxation rate vs. V data will be made in the Discussion.

Fig. 4 summarizes data that compare the mean values of Q_s(on) and Q_s(off) for measurements at voltages between -160 and $+60$ mV under four experimental

conditions of Na addition or removal (90 Na, 45 Na, 120 Na, and hypertonic 90 Na). The condition Q_s(on) = Q_s(off) is well met except for the group of data at the most extreme negative values of membrane potential, where Q_s(on) tends to be less than Q_s(off). Q_s meets the three requirements for a "membrane charge movement" process (Chandler, Rakowski, and Schneider, 1976): (*1*) voltage-dependent relaxation rate, (*2*) saturating sigmoid voltage dependence of the quantity of charge moved, and (*3*) equality of on and off charge moved (with the exception noted above). The phenomenon described here, however, is not related to excitation–contracting coupling or ionic channel gating currents. The principal characteristic that is different is the voltage independence of the relaxation rate at positive values of membrane potential (Fig. 3 C).
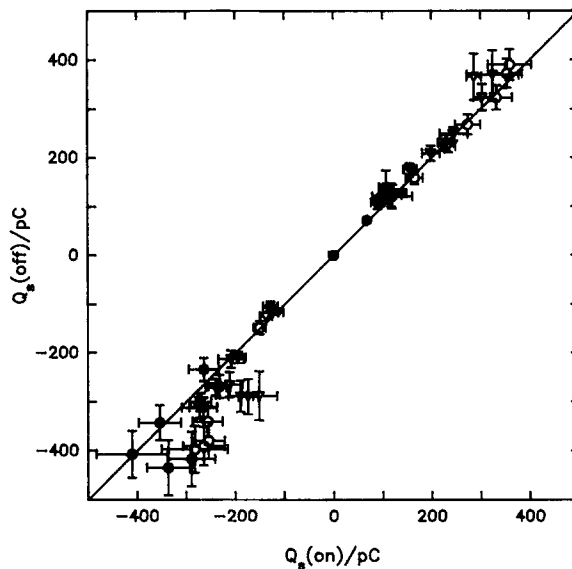

FIGURE 4. Equality of on and off slow charge movement. The mean values of Q_s(on) and Q_s(off) are plotted (± SEM) for various membrane potentials between −160 and +60 mV and for four different experimental changes to Na-free solution. *Filled circles*, 90 Na; *open circles*, 45 Na; *filled triangles*, 120 Na; *open triangles*, hypertonic 90 Na. The solid line is the theoretical relationship Q_s(on) = Q_s(off).

Comparison of Difference Current Records Obtained upon Na Addition with Those Obtained upon Na Removal

Fig. 5 shows a comparison of difference current records obtained by a solution change from Na-free solution to 90 Na (Fig. 5 *A*) and records subsequently obtained in the same oocyte upon changing from 90 Na back to Na-free solution (Fig. 5 *B*). Except for the data that are sampled during the capacitive transient (4–6 ms after each step), the time course of the decline in current and the magnitude of the difference current records are quite similar. Fig. 5, *C* and *D*, shows that the values of Q_{off} and the relaxation rates are very similar for the Na addition and Na removal data. The data, therefore, demonstrate not only that the slow component of Na-sensitive charge movement is reversible, but also that the major features of the data are reproducible regardless of the sequence in which the control and test records are obtained. The
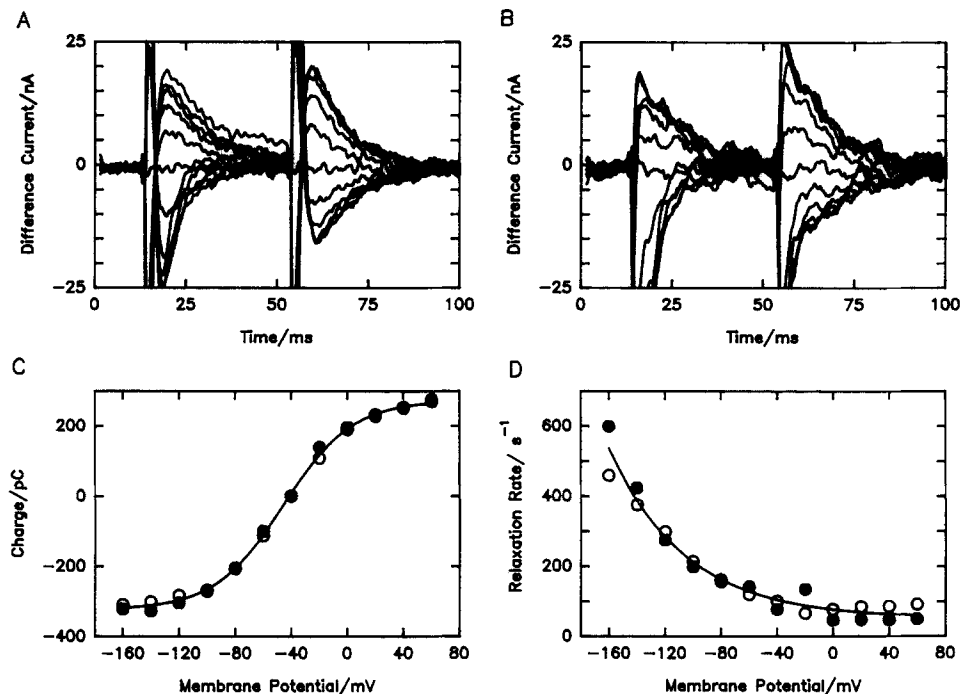
FIGURE 5.   Comparison of the slow component of Na-sensitive current determined by addition or removal of extracellular Na$^+$. (A) Difference current records obtained in an oocyte upon changing from Na-free solution to 90 Na. (B) Difference current records obtained in the same oocyte for a subsequent change from 90 Na to Na-free solution. (C) Comparison of Q_{off} for the Na addition data in A (filled circles) with Q_{off} measured from the Na removal data in B (open circles). The solid line is drawn according to Eq. 2, with least-squares parameters Q_{smin} = −324 ± 5 pC, Q_{stot} = 599 ± 9 pC, z_q = 1.03 ± 0.04, and V_q = −45.3 ± 0.9 mV. (D) Comparison of the current relaxation rates for the Na addition data (filled circles) with those measured by Na removal (open circles). The solid line is drawn according to Eq. 1 with least-squares parameters a_k = 51 ± 14 s^{-1}, z_k = 0.47 ± 0.05, and V_k = −38 ± 27 mV. Before recording the data in A, an initial set of difference current records was obtained upon Na removal that had a fast component of current that was not present in any subsequent set of records.

ability of the cardiotonic steroid dihydroouabain (DHO) to block the pre–steady-state current is examined below.

Characteristics of the Slow Component of DHO-sensitive Current

Difference current records obtained from an oocyte in which 100 μM DHO was added to the 90 Na bathing solution are shown in Fig. 6A. The magnitude and general characteristics are similar to the Na-sensitive difference currents shown in Figs. 3A and 5, A and B. It is important to note that both the Na-sensitive transient current shown in Figs. 3A and 5, A and B, as well as the DHO-sensitive transients shown in Fig. 6A decline to the same steady-state level during the voltage pulse as

was measured before the pulse. This directly shows that there was no measurable Na- or DHO-sensitive current in the steady state at any voltage, and rules out any significant contribution to the transient current of any electrogenic mode of operation of the Na/K pump under these experimental conditions. Considering the noise
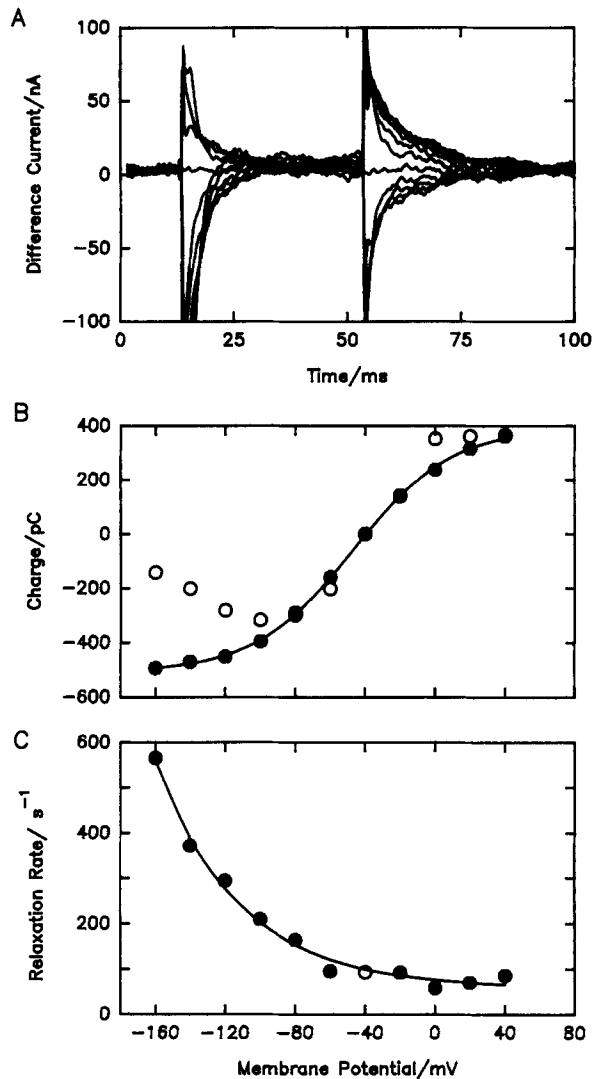

FIGURE 6. DHO-sensitive transient current. (*A*) The difference current obtained by subtraction of signal-averaged current records in 90 mM Na, K-free solution before and 5 min after the addition of 100 μM DHO. Command voltage pulse protocol as in Fig. 1 *A*. (*B*) Voltage dependence of the DHO-sensitive Q_s(on) (*open circles*) and Q_s(off) (*filled circles*) calculated from the exponential fit to the current records in *A*. The line is calculated from the least-squares fit to the filled symbols according to Eq. 2, where Q_{smin} = −510 ± 6 pC, Q_{stot} = 906 ± 13 pC, z_q = 0.891 ± 0.027, and V_q = −46.6 ± 0.8 mV. (*C*) Voltage dependence of the relaxation rate of the slow component (k_s) of DHO-sensitive current. *Filled symbols*, relaxation rates calculated from difference current records in *A* during the voltage pulse (on). *Open symbol*, relaxation rate calculated from data during the off period of time in *A*. The SEM is smaller than the symbol radius. The solid line is the best fit of the data to Eq. 1, with a_k = 58 ± 11 s⁻¹, z_k = 0.53 ± 0.05, and V_k = −56 ± 18 mV.

level of the data, such electrogenic modes of pump operation could amount to no more than ~10% of the peak transient current magnitude. The voltage dependence of the DHO-sensitive charge and relaxation rates are shown in Fig. 6, *B* and *C*. These data are similar in all respects to the data obtained by Na removal. A more direct comparison of the data is shown in Fig. 7.

Direct Comparison of Na-sensitive and DHO-sensitive Currents

Fig. 7 is a summary of all of the data obtained from 10 oocytes in which changes between 90 Na and Na-free solution were made and 7 oocytes in which 100 μM DHO was added to the 90 Na bathing solution. The solid line represents a least-squares fit to the DHO data. The value of V_q was determined to be -40.3 ± 0.5 for the DHO data and -40.8 ± 0.6 for the data obtained by Na removal. The values are not significantly different ($P > 0.5$). The overall estimate of the parameter Q_{stot} was 946 ± 10 pC for the DHO data and 809 ± 7 pC for the Na removal data. This difference in magnitude may be accounted for by less-than-complete Na removal. The apparent valence (z_q) was fixed at a value of 1.0 for the final fit procedure since it did not differ significantly from 1.0 for either set of data.

The mean values of k_s measured by DHO addition or Na removal are shown in Fig. 7 *B*. The fits to these individual sets of data did not differ significantly, so they were combined to give an overall estimate of the value of $a_k = 99.5 \pm 0.3$ s^{-1}, $z_k = 0.44 \pm 0.07$, and $V_k = -49.7 \pm 3.4$ mV. The conclusion from the data in Fig. 7 is that the characteristics of the DHO- and Na-sensitive difference currents are indistinguishable. We also conclude from the characteristics described above and its sensitivity to DHO that the pre–steady-state transient current measured here represents membrane charge movement mediated by extracellular Na-sensitive partial reactions of the Na/K pump that produce no steady-state current.

Effect of Changes in [Na] on the Voltage Dependence of Q_s and k_s

Nagel, Suenson, Nakao, and Gadsby (1991) have reported that the Q vs. V and k vs. V relationships are shifted to more positive potentials by increasing extracellular [Na] in cardiac myocytes. The effect of the test external [Na] on the voltage dependence of Q_s and k_s in *Xenopus* oocytes is shown in Fig. 8. Q_s(off) data measured by subtraction of control current records in Na-free solution from test records in 45 Na were normalized and fit by Eq. 2 with z_q set to 1.0 and gave a least-squares value of -65.5 ± 1.4 mV for the parameter V_q. Compared with the mean value of -40.8 ± 0.6 measured in 90 Na, there is a shift of V_q of -24.7 ± 2.0 mV upon halving [Na]. Similarly, there is a shift of -26 ± 11 mV of the parameter V_k used to describe the voltage dependence of the relaxation rate.

A shift of V_q in the opposite direction is observed when comparing Q_s measurements in hypertonic 90 Na with those in 120 Na. Fig. 9 *A* shows the mean value of the normalized Q_s data. The value of V_q in hypertonic 90 Na is -46.7 ± 0.8 mV and in 120 Na is -31.9 ± 1.4 mV, giving a shift of $+14.8 \pm 2.2$ mV for this 33% increase in [Na]. The relaxation rate data, however, did not shift in parallel. As shown in Fig. 9 *B*, the mean values of V_k and k_s were unchanged in hypertonic 90 Na and 120 Na. This result is unexpected and is not explained by the models discussed below.

DISCUSSION

Modes of Operation of the Na/K Pump

In the absence of extracellular K$^+$ the Na/K pump may still operate in several alternative modes. For example, it is possible for the Na/K pump to engage in
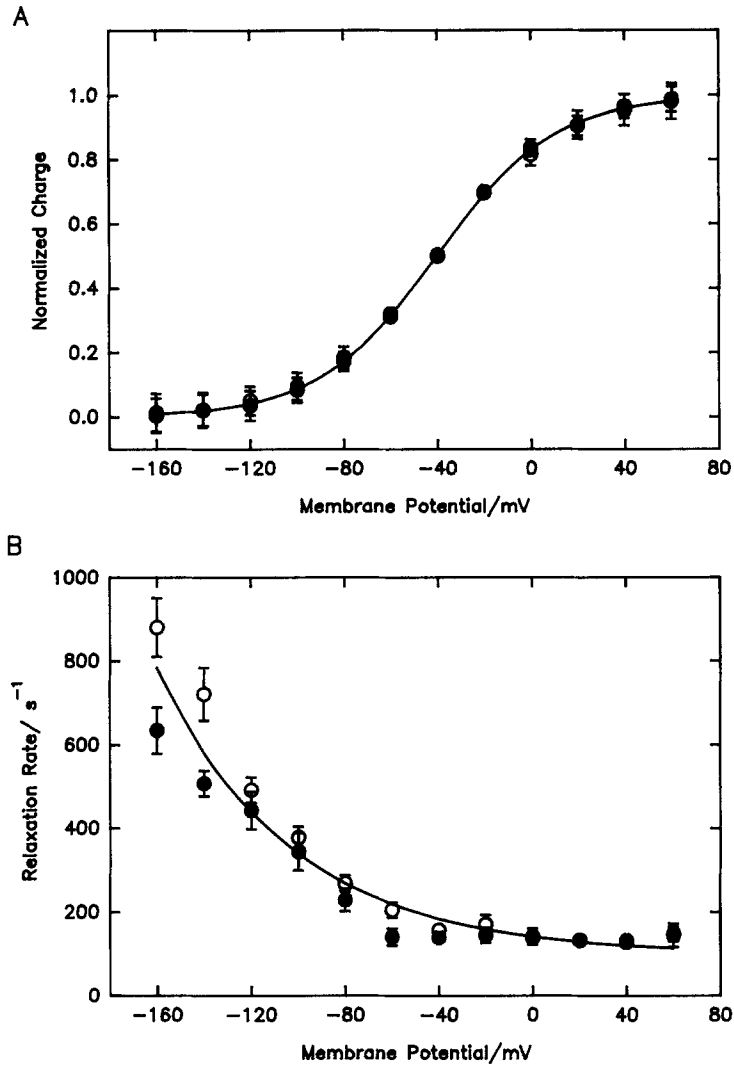
A

Normalized Charge

1.0
0.8
0.6
0.4
0.2
0.0

−160   −120   −80   −40   0   40   80
Membrane Potential/mV

B

1000

Relaxation Rate/ s^{-1}

800

600

400

200

0

−160   −120   −80   −40   0   40   80
Membrane Potential/mV

FIGURE 7. Comparison of the voltage dependence of the slow component of pre–steady-state charge movement (Q_s) and its relaxation rate (k_s) measured either as DHO-sensitive or Na-sensitive current. (A) Voltage dependence of Q_s in 90 mM Na solution. *Filled circles*, mean values of Q_s(off) calculated from DHO-sensitive current records in seven oocytes, normalized to the least-squares values of Q_{smin} = −473 ± 6 pC, and Q_{stot} = 946 ± 10 pC. The fit to the mean values gave z_q = 0.966 ± 0.024, close to 1.0, so that the normalized data in A could be fit with z_q = 1.0 according to Q_{snorm} = $1/\{1 + \exp[z_q(V_q - V)F/RT]\}$, in which the only remaining free parameter V_q was found by least-squares analysis to be −40.3 ± 0.5 mV. *Open symbols*, mean values of Q_s(off) calculated from the Na-sensitive current records from 21 determinations in 10 oocytes (14 measurements made by changing from 90 Na to Na-free solution and 7 measurements made by addition of 90 Na to Na-free solution). The magnitudes of the least-squares fit parameters for the Na-sensitive charge were Q_{smin} = −408 ± 4 pC, Q_{stot} = 808 ± 7 pC, and z_q = 1.01 ± 0.02. The normalized data were fit with z_q set to 1.0 and yielded a least-squares value of V_q = −40.8 ± 0.3. The solid line is drawn with a value of V_q = −40.5 mV. The solid symbols obscure the open symbols. (B) Voltage dependence of the relaxation rate of the slow component of difference current in 90 mM Na. *Filled symbols*, relaxation rates determined from difference current records obtained before and after DHO addition. *Open symbols*, relaxation rates determined from difference current records upon addition or removal of 90 mM Na. The solid line is the least-squares fit to both sets of data according to Eq. 1 with a_k = 99.5 ± 0.3 s^{-1}, z_k = 0.44 ± 0.07, and V_k = −49 ± 3 mV.
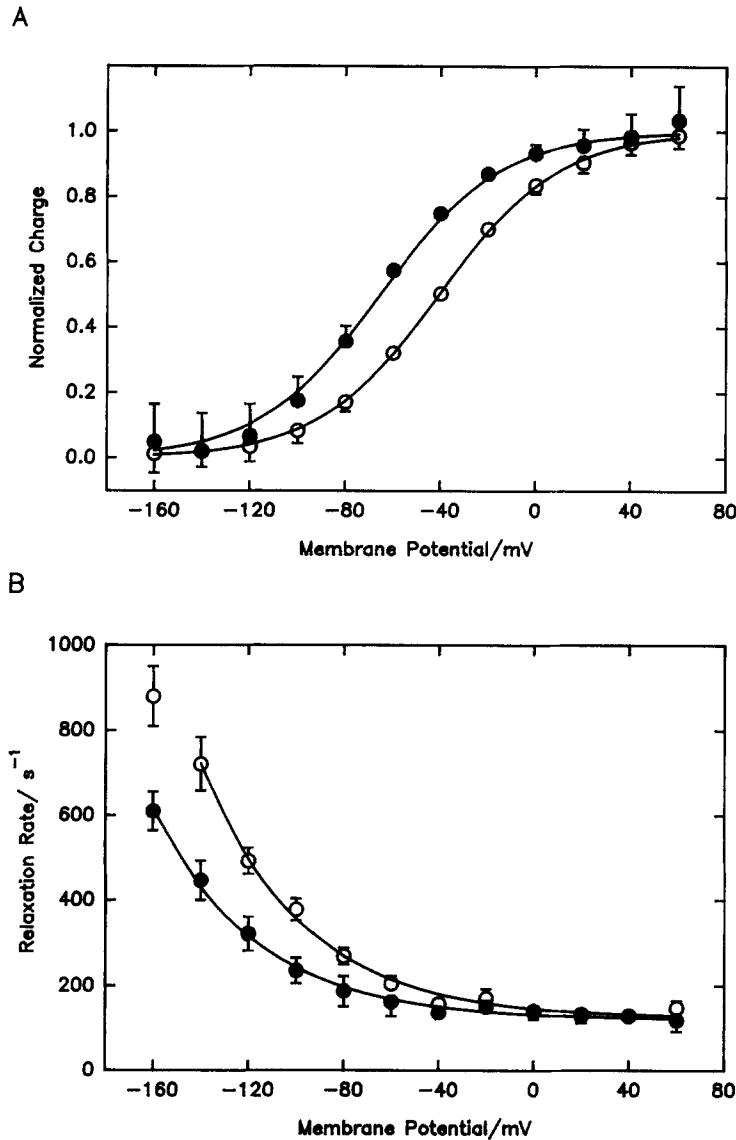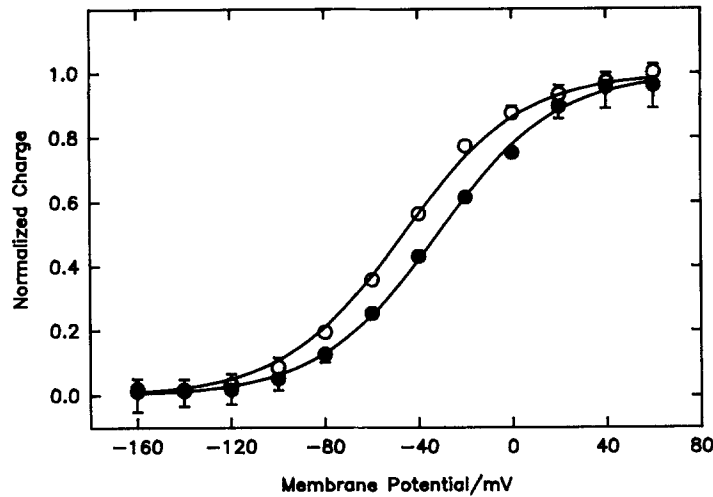
FIGURE 8. Effect of reducing external [Na$^+$] from 90 to 45 mM on the voltage dependence of Q_s and k_s. (A) Voltage dependence of Q_s in 90 and 45 mM external [Na$^+$]. Open symbols, data from Fig. 7 at 90 mM [Na$^+$]. Filled symbols, normalized Q_s measured from five oocytes upon changing from 45 mM [Na$^+$] to Na-free solution and in five oocytes upon addition of 45 mM [Na$^+$] to Na-free solution. The least-squares fit parameters used for normalization were Q_{smin} = −447 ± 12 pC, Q_{stot} = 597 ± 17 pC, and z_q = 1.10 ± 0.09. The value of z_q was set to 1.0 for the fit to the normalized data and gave a value of V_q = −65.5 ± 1.4 mV for the final remaining free parameter. The estimate of the shift in V_q produced by halving [Na$^+$] is, therefore, −24.8 ± 1.7 mV. (B) Voltage dependence of k_s in 90 and 45 mM external [Na$^+$]. Open symbols, k_s determined in 90 mM [Na$^+$] upon addition or removal of Na$^+$ from Fig. 7 B. The least-squares parameters for these data over the voltage range from −140 to +60 mV are a_k = 124 ± 8 s^{-1}, z_k = 0.598 ± 0.035, and V_k = −73 ± 7 mV. Filled symbols, k_s determined in 45 mM [Na$^+$]. The least-squares parameters are a_k = 120 ± 5 s^{-1}, z_k = 0.591 ± 0.028, and V_k = −99 ± 5 mV. The estimate of the shift in V_k produced by halving the [Na$^+$] is, therefore, −26 ± 12 mV.
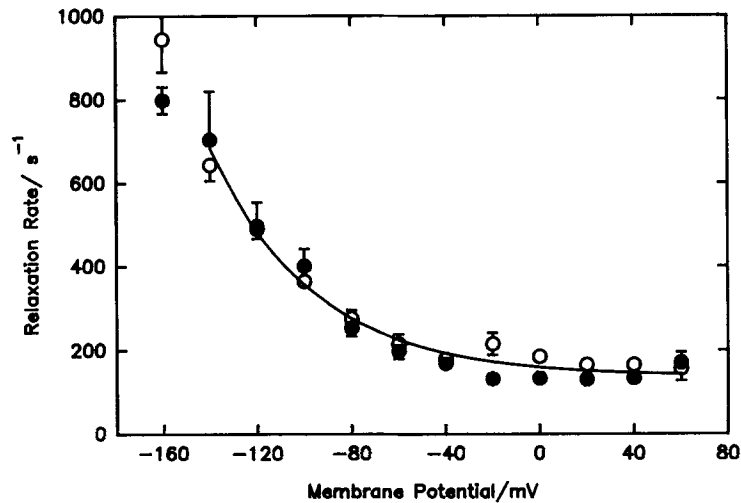
A

B

FIGURE 9. Effect of raising external [Na$^+$] from 90 to 120 mM under hypertonic conditions. (A) Voltage dependence of Q_s(off). *Open symbols*, data from 11 oocytes in which hypertonic 90 mM Na was exchanged with hypertonic Na-free solution, eight determinations were made upon Na$^+$ removal, and five were made upon Na$^+$ addition. The least-squares parameters from the fit to the mean value at each voltage were Q_{smin} = −320 ± 4 pC, Q_{stot} = 567 ± 7 pC, and z_q = 1.09 ± 0.04. The data were normalized and refit with z_q = 1.0, giving a least-squares value of V_q = −46.7 ± 0.9 mV for the equation of the line through the open symbols. *Filled symbols*, data from 12 oocytes in which 120 mM Na was exchanged with hypertonic Na-free solution, nine determinations upon Na$^+$ removal, and seven upon Na$^+$ addition. The least-squares fits to the mean values were Q_{smin} = −302 ± 7 pC, Q_{stot} = 699 ± 15 pC, and z_q = 0.992 ± 0.052. The normalized data were fit with z_q set to 1.0 and gave a final least-squares value of V_q = −31.9 ± 0.7 mV for the equation of the line drawn through the filled symbols. The shift in V_q produced by changing from hypertonic 90 mM [Na$^+$] to 120 mM [Na$^+$] was, therefore, +14.7 ± 1.7 mV. (B) Voltage dependence of k_s in hypertonic 90 and 120 mM [Na$^+$]. *Open symbols*, mean values of k_s measured in the 11 oocytes from A in hypertonic 90 mM [Na$^+$]. *Filled symbols*, mean values of k_s measured in the 12 oocytes examined in 120 mM [Na$^+$]. The least-squares fits to the open and filled symbols were not significantly different, so the data were combined and gave the following values of least-squares parameters for the line through the data: a_k = 138 ± 11 pC, z_k = 0.58 ± 0.05, and V_k = −79.6 ± 8.6 mV.

electrogenic $3Na^+/2Na^+$ exchange (Lee and Blostein, 1980), $3Na^+/2Na^+$ exchange (Polvani and Blostein, 1988), uncoupled ATP-dependent Na^+ extrusion (Garrahan and Glynn, 1967a; Cornelius, 1989), reverse $2K^+/3Na^+$ pumping (Garrahan and Glynn, 1967c), and ADP-dependent electroneutral $3Na^+/3Na^+$ exchange (Garrahan and Glynn, 1967b; Abercrombie and De Weer, 1978). Of all the possibilities, only those that are electroneutral and thus produce no steady-state current are compatible with the observation in Fig. 6 A that there is no significant steady-state DHO-sensitive current under these experimental conditions. The most likely explanation is that intracellular [ADP] in oocytes is sufficient to allow the partial reactions of the pump cycle responsible for electroneutral ADP-dependent $3Na^+/3Na^+$ exchange to occur, as is the case in normal human red blood cells. Despite the fact that the net exchange reaction is electroneutral, pre–steady-state transient currents can occur as a result of the voltage-dependent redistribution of charge. The enzyme intermediates involved in Na/Na exchange might themselves be charged and directly produce translocation of charge within the membrane field. However, the recent data of Gadsby, Rakowski, and De Weer (manuscript submitted for publication) on the voltage dependence of unidirectional Na efflux mediated by electroneutral Na^+/Na^+ exchange (presumably $3Na^+/3Na^+$ exchange) has established that the voltage dependence arises principally or exclusively in the extracellular Na^+ binding rate constant. These authors suggest that this is a consequence of the existence of a channel-like extracellular ion well for Na^+ in the Na/K pump molecule. In this model charge translocation takes place exclusively within the extracellular access channel. Their model for the voltage dependence of the operation of the Na/K pump has been adopted and extended in the Appendix to account for several of the properties of the measured pre–steady-state membrane charge movement.

Comparison of the Magnitude and Apparent Valence of Q_s with Charge Movement Measurements in Myocytes

The most striking agreement between the characteristics of Q_s measured in *Xenopus* oocytes and strophanthidin-sensitive charge movement measured in guinea pig myocytes (Nakao and Gadsby, 1986) is the steepness of the charge vs. voltage relationship. Nakao and Gadsby found an e-fold steepness factor of 26.5 mV, which corresponds to an apparent valence of 1.01 (RT/F = 26.73 mV at 37°C). All of the normalized charge data in Figs. 7–9 are well fit by an apparent valence (z_q) of 1 under all of the experimental conditions examined. The apparent valence may be expressed as the product of three terms as follows:

$$z_q = nq\delta \tag{3}$$

where n is the apparent molecularity of (effective number of ions involved in) the slow charge movement process, q is the valence of the charged species, and δ is the fraction of the membrane field over which the charge translocation takes place. Since $z_q = 1$, the simplest hypothesis is that the slow charge movement process represents the transolcation of one Na^+ through the entire membrane field. The remaining two Na^+ ions may be translocated in an electrically silent fashion consistent with the suggestion of Gadsby and Nakao (1986) that the enzyme has two negatively charged ion binding sites. Based on the assumption of one net charge moved per pump site,

we may calculate a pump site density. From the values of Q_{stot} for the DHO-sensitive and 90 Na data and a value of 0.18 μF of linear capacitance per oocyte (Vasilets, Omay, Ohata, Noguchi, Kawamura, and Schwarz, 1991), the slow component of charge in *Xenopus* oocytes is in the range 4.5–7.0 nC μF^{-1}, which corresponds to a pump site density of 270–420 sites μm^{-2} (assuming a value of specific capacitance of 1 $\mu F\ cm^{-2}$). These values are in good agreement with the values of 330–360 ouabain binding sites μm^{-2} measured by Vasilets et al. (1991). Nakao and Gadsby (1986) measured a total quantity of movable charge of 19 nC μF^{-1}, from which they calculated a pump site density of 1,200 μm^{-2} in ventricular myocytes.

Comparison of Midpoint Voltages

Nakao and Gadsby (1986) found a midpoint voltage of the steady-state charge distribution function of −20 mV. This value is somewhat more positive than the values of V_q of −40.3 ± 0.5 and −40.8 ± 0.6 found for the DHO and 90 Na data, respectively. However, as shown in Figs. 8 and 9, V_q is a function of [Na]. In addition, one would not expect the values of V_q from different species to be in agreement since it may be affected by such factors as the surface charge of the different membranes.

Comparison of the Values of k_s and Its Voltage Dependence

The shape of the relaxation rate vs. voltage relationship in cardiac myocytes is very similar to the k_s vs. voltage relationships shown in Figs. 3 and 5–9. The relaxation rate approaches a constant value for large depolarizations and increases exponentially with hyperpolarization. Nakao and Gadsby (1986) find a value of $\sim 250\ s^{-1}$ at −20 mV and 37°C. The value of the relaxation rate at −20 mV in *Xenopus* oocytes was found to be $\sim 180\ s^{-1}$ (Fig. 7) (temperature, 22°C). This value is in reasonable agreement with that of Nakao and Gadsby (1986), considering the difference in temperature between the two sets of experiments.

The exponential steepness factor, z_k, was found to be 0.41 ± 0.07 for the DHO data and 0.60 ± 0.04, 0.60 ± 0.03, 0.58 ± 0.05, and 0.58 ± 0.06 for the 90 Na, 45 Na, 120 Na, and hypertonic 90 Na data, respectively. Nakao and Gadsby (1986) did not fit their relaxation rate data to a theoretical function, but an estimate obtained from their data by De Weer (1990) is 0.38 ± 0.07. A reasonable tentative conclusion is that z_k obtained from a simple exponential fit of the data is ~ 0.5, while z_q is 1.0.

Alternative Models of Charge Translocation during a Half-Cycle of Na/Na Exchange

The interpretation of their data proposed by Nakao and Gadsby (1986) is straightforward. They proposed that there are two negatively charged Na^+ binding sites on the Na/K pump molecule, so that the pump has a single net positive charge when three Na^+ are bound. The rate of charge translocation should then depend on membrane voltage with depolarization increasing the forward rate coefficient and decreasing the backward rate coefficient and hyperpolarization having the opposite effect. The midpoint potential of the steady-state charge distribution function is the voltage at which the forward and backward rate coefficients are equal. They also raised the possibility that the voltage-dependent transition might correspond to the conformational change of the phosphorylated, occluded-Na intermediate:

$E_1P \cdot (Na_3)$ − E_2PNa_3. Indeed, there is a general assumption in the literature (Glynn, 1984) that this conformational change is likely to be the charge-translocating, voltage-dependent step. However, recent evidence on the voltage dependence of Na efflux mediated by electroneutral Na/Na exchange (Gadsby, D. C., R. F. Rakowski, and P. De Weer, manuscript submitted for publication) has led to the conclusion that only external Na binding rate coefficients are voltage dependent, which implies that Na ions reach their external binding sites through a high field access channel (ion well) (Mitchell and Moyle, 1974; Lagnado, Cervetto, and McNaughton, 1988).
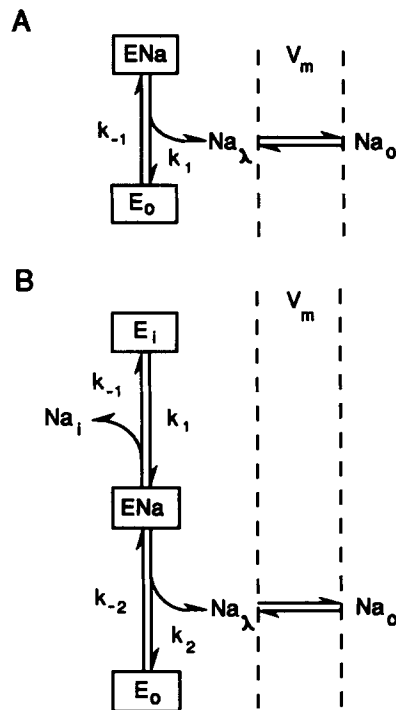

FIGURE 10. Pseudo two-state and pseudo three-state models of pre–steady-state membrane charge movement. (A) Pseudo two-state model. The translocation of two Na^+ is assumed to be electrically silent. One Na^+ is bound and occluded at the internal face of the enzyme and is released into an external high field access channel (ion well). Only the rate constants for transitions between the Na-bound and occluded state (ENa) and the Na-unbound state in the external facing conformation of the enzyme (E_0) are considered in this model. The forward rate constant (k_1) is assumed to be voltage independent, while the reverse pseudo first-order rate coefficient (k_{-1}) is voltage dependent as a consequence of the membrane voltage (V_m) acting to alter the effective [Na] at the ion binding locus (λ) according to a Boltzmann equilibrium within an external access channel that extends through the entire membrane field. (B) Pseudo three-state model. Transitions between ENa and E_0 are governed by a voltage-independent forward rate constant (k_2) and a voltage-dependent pseudo first-order reverse rate coefficient (k_{-2}) as in A. The model is extended to include consideration of voltage-independent transitions between ENa and a third state (E_i) that is inward facing and to which internal Na may bind with a pseudo first-order forward rate coefficient (k_1). The rate of reverse occlusion/unbinding from ENa is governed by a voltage-independent rate constant (k_{-1}).

Fig. 10 is an illustration of two alternative models of the half-cycle of Na/Na exchange by the Na/K pump. Fig. 10 A is similar to the models previously considered by Nakao and Gadsby (1986), Läuger and Apell (1988), De Weer (1990), and Läuger (1991), except that only the reverse rate coefficient (k_{-1}) is assumed to be voltage dependent, deriving its voltage dependence from the equilibrium between the effective concentration of Na at its binding locus, $[Na]_\lambda$, and its concentration in the external medium, $[Na]_0$. As shown by the derivations in the Appendix, this model predicts shifts in the midpoint voltages of both the charge and rate coefficient relationships with changes in $[Na]_0$. However, the model is inconsistent with the data

in that it requires that the e-fold steepness factors for charge (z_q) and for the rate coefficient data (z_k) be equal (as previously discussed by De Weer, 1990).

Fig. 10 B is a simple extension of the pseudo two-state model. Rather than resulting in a simple forward voltage-independent rate constant and exponentially voltage-dependent reverse rate coefficient, this pseudo three-state model predicts forward and reverse rates k_f and k_b that are composed of all four rate coefficients of the model (see Eqs. A32 and A33 in the Appendix). These forward and backward rates obey a sigmoid distribution in which the exponential steepness factor (z_k) is the same as for the steady-state charge distribution function (z_q), but since the maximum values of k_f and k_b may, in general, be different, the midpoint voltage of the sigmoid curve governing the forward and backward rates (V_{fb}) is different from V_q (cf. Eqs. A37 and A22). This does not eliminate the requirement that V_q correspond to the voltage (V_k) at which k_f equals k_b (Eq. A29).

Uniqueness of the Determination of Model Parameters

The derivations in the Appendix illustrate certain common features of the class of kinetic models in which only a single terminal Na rebinding rate coefficient is exponentially voltage dependent. The identical form of the equations for the steady-state Q vs. V relationship for the pseudo two-state (Eq. A7) and pseudo three-state models (Eq. A21) illustrates a general property of models of this class, namely, that the quantity of charge moved obeys a sigmoid steady-state Boltzmann distribution as a function of voltage. Sufficient information is available in the data to uniquely determine the values of total charge (Q_{tot}), exponential steepness (z_q), and the midpoint voltage of the distribution (V_q), and if experiments are done at various [Na] the data allow an estimate of the access channel depth (δ) to be obtained; however, additional independent information is needed to uniquely determine the individual rate constants of the underlying model.

Equality of Q (on) and Q (off)

Both the pseudo two-state and pseudo three-state models predict equality of the on and off quantity of charge moved in response to a voltage step as indicated by the theoretical line of equality in Fig. 4. Strict charge conservation, however, is not a general property that is required for all members of the general class of access channel models being considered. Failure to observe equality of on and off areas may result, for example, from kinetically trapping enzyme intermediates in states from which recovery is either too slow or too fast to be seen within the time resolution of the measurements. The observation in Fig. 4 that Q (on) tends to be less than Q (off) for steps to hyperpolarized potentials, might, however, simply be a result of underestimation of Q (on). The extrapolation procedure used to calculate the quantity of charge moved would tend to fail as the relaxation rate increased, and therefore could account for a larger error at hyperpolarized potentials. This possibility has recently been reexamined by Holmgren and Rakowski (1993), who found good agreement of Q (on) and Q (off) at all voltages when direct numerical integration was used to calculate the quantity of charge moved. This equality of Q (on) and Q (off) was also found to be independent of holding potential in the range -100–0 mV.

Fit of the Pseudo Three-State Model to the Charge and Rate Coefficient Data of Fig. 6

Fig. 11 shows that the pseudo three-state model is capable of being fitted to charge and relaxation rate data obtained from DHO-sensitive transient currents using a single set of self-consistent rate coefficients. Unfortunately, the fit is not unique since the model requires seven free parameters, more than can be extracted from this data set. The overspecification of the model results from the loss of information contained in the time course of the predicted rising phase of the current transient (Eq. A23). Comparison of Eqs. A8 and A22 in the Appendix shows that the pseudo two-state and pseudo three-state models predict the same shift in V_q with changes in $[Na]_0$ (Eq. A9), so that these two models cannot be distinguished based on the shift of V_q. One way to choose between the models is to obtain data in which the rising phase of the transient membrane charge movement (if any) is resolved. This may be possible either in voltage-clamped squid giant axons or in *Xenopus* oocytes that are voltage clamped with an improved technique (Taglialatela, Toro, and Stefani, 1992).

Shift in V_q with Changes in $[Na]_0$

The data in Fig. 8 give a shift of -24.8 ± 1.7 mV in the value of V_q for a change from 90 to 45 mM $[Na]_0$. Similarly, the value of ΔV_q obtained from Fig. 9 on changing from hypertonic 90 to 120 mM $[Na]_0$ is $+14.7 \pm 1.7$ mV. We may calculate the apparent depth of the external access channel for Na (δ) from these data by application of Eq. A9: δ is in the range 0.5–0.7 and represents the fraction of the membrane field sensed by Na between the bulk solution and its external binding site. Sagar, Wallner, and Rakowski (1993) have obtained a value of 0.75 ± 0.02 based on the shift in the I-V relationship of the forward-going Na/K pump in *Xenopus* oocytes produced by changes in external [Na], and De Weer, Gadsby, and Rakowski (1993) have reported an estimate of ~ 0.67 based on external [Na]-dependent shifts in the backward-running I-V relationship and in the Na efflux vs. voltage relationship of Na/K pump–mediated Na/Na exchange in squid giant axons. The simple assumption that since $z_q = 1.0$ the slow charge movement process represents the movement of one net charge through the entire membrane field is probably not warranted. A value of $z_q = 1.0$ could arise, for example, from an apparent Hill coefficient of $n = 1.5$ and an access channel depth of $\delta = 0.67$.

Estimates of Q_{tot} for Various $[Na]_0$

An observation that is not predicted by either the pseudo two-state or pseudo three-state model is that the measured value of Q_{tot} increases as $[Na]_0$ is increased. At 45 mM Na_0 $Q_{stot} = 597 \pm 17$ pC (Fig. 7 A), while at 90 mM Na_0 $Q_{stot} = 808 \pm 7$ pC. (Fig. 6 A). In hypertonic 90 Na $Q_{stot} = 567 \pm 7$ pC, while in hypertonic 120 Na $Q_{stot} = 699 \pm 15$ pC (Fig. 8). Neither of the models considered here predicts a change in Q_{stot} with changes in $[Na]_0$. A possible explanation might be that increasing $[Na]_0$ is able to recruit more enzyme to participate in the slow electrogenic reactions from a nonparticipating pool.
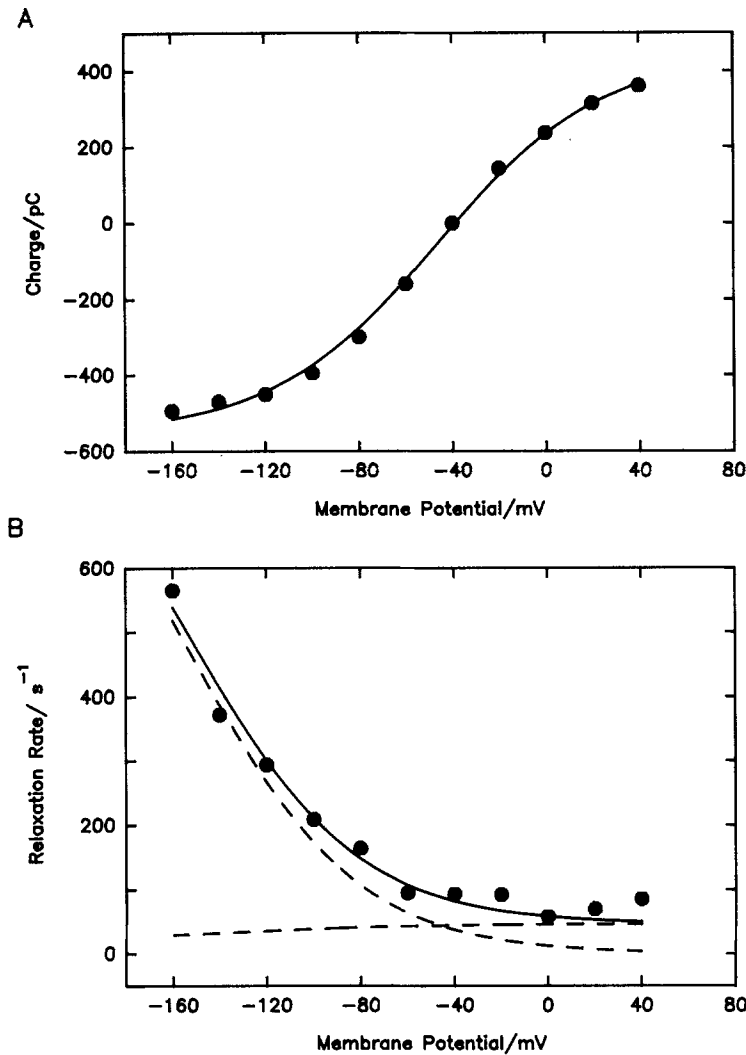
FIGURE 11. Least-squares fit of the pseudo three-state model to the charge and rate coefficient data from Fig. 6. (A) Charge data from Fig. 6 B. Rate coefficient data from Fig. 6 C. The solid lines represent a simultaneous least-squares fit to both sets of data by Eqs. 2 (data in A) and A27 (data in B). The values of the seven free parameters of the pseudo three-state model are the following: q_{min} = −550 pC, q_{tot} = 1,000 pC, z_q = 0.72, k_1 = 760 s^{-1}, k_{-1} = 175 s^{-1}, k_2 = 60 s^{-1}, and $k_{-2}(0)$ = 150 s^{-1} M^{-1}. The solid lines show the fit to the data. The dashed lines represent the forward and backward rate coefficients as described by Eqs. A32 and A33 in the Appendix. This set of parameters meets the requirement for the application of Eq. A27 that $4C_2/C_1^2 \ll 1$ well at a V_m of 0 mV, but somewhat less well as V_m is made more negative.

Testable Predictions of the Pseudo Three-State Model

Some of the testable predictions of the pseudo three-state model are the following: (1) the pre–steady-state transient charge movement should have a rising phase, (2) the midpoint voltages V_q and V_{fb} may differ (cf. Eqs. A22 and A37), but the e-fold steepness factors z_q and z_k should be the same if the proper expression is used to fit the relaxation rate data, (3) the backward rate coefficient should approach a limiting value at hyperpolarized potentials (this may be possible to see by shifting the Q and k vs. V curves to the right by using very high external [Na]), (4) the magnitude of the shift in V_q and V_k should be predicted by Eq. A9, and (5) Q_{tot} should be constant and, in particular, independent of [Na]$_0$.

APPENDIX

Pseudo Two-State Model of Na Translocation

The two-state charge translocation model previously described (Nakao and Gadsby, 1986; De Weer, 1990) can readily be modified to accommodate the presence of an external high-field access channel for Na. Following Läuger and Apell (1988), we may write a pseudo two-state reaction scheme (Fig. 10 A) in which the forward rate constant for the transition from the Na-occluding enzyme state (ENa) to the external-facing enzyme state (E_0) is given by a first-order voltage-independent rate constant (k_1). The pseudo first-order reverse rate constant (k_{-1}) is equal to $k_{-1}(0)$ [Na]$_\lambda$, where $k_{-1}(0)$ is the second-order rate constant for the transition from E_0 to ENa, and [Na]$_\lambda$ represents the effective [Na] at the ion binding locus within the external high field access channel.

Assuming that the rate constants for traversing the external ion well are rapid, we may write a Boltzmann expression for the equilibrium distribution of Na between the external medium ([Na]$_0$) and its binding locus:

$$[Na]_\lambda^n = [Na]_0^n \exp (-z_k FV/RT) \tag{A1}$$

The symbol z_k represents an apparent valence, $z_k = z_q$, as defined by Eq. 3, V is the membrane potential, n is the Hill coefficient for Na, and F/RT has its usual meaning. The expression for k_{-1} is, therefore,

$$k_{-1} = k_{-1}(0)[Na]_0^n \exp (-z_k FV/RT) \tag{A2}$$

The time course of the initial equilibrium redistribution of Na$^+$ between Na$_0$ and Na$_\lambda$ after a voltage step is assumed to be too rapid to be measured by the recording apparatus. Since Na$^+$ is bound to and released from the state E_0, the time course of E_0 determines the time course of charge translocation ($Q(t)$) and the pre–steady-state current ($I(t)$) is proportional to d$E_0(t)$/dt. We may write the differential equations for the reaction scheme, define a total amount of enzyme (E_{tot}), and solve for $E_0(t)$ for the initial condition $E_0(0) = 0$ to give

$$E_0(t) = \frac{k_1 E_{tot}}{k_1 + k_{-1}} \{1 - \exp [-(k_1 + k_{-1})t]\} \tag{A3}$$

Steady-State Charge Distribution for the Pseudo Two-State Model

The first term of Eq. A3 is the steady-state solution, so that the steady-state charge ($Q(V, \infty)$) normalized to the total charge (Q_{tot}) may be written

$$\frac{Q(V, \infty)}{Q_{tot}} = \frac{k_1}{k_1 + k_{-1}} \tag{A4}$$

We may substitute Eq. A2 and Eq. A4 and rearrange to obtain the steady-state voltage and external [Na] dependence:

$$\frac{Q(V, \infty)}{Q_{tot}} = \frac{1}{1 + \left(\frac{k_{-1}(0)[Na]_0^n}{k_1}\right) \exp\left(\frac{-z_k FV}{RT}\right)} \tag{A5}$$

We now define a midpoint voltage of the steady-state charge distribution (V_q) such that

$$\frac{k_{-1}(0)[Na]_0^n}{k_1} = \exp\left(\frac{z_k FV_q}{RT}\right) \tag{A6}$$

Substituting Eq. A6 in Eq. A5, we obtain the following steady-state Boltzmann relationship for membrane charge:

$$\frac{Q(V, \infty)}{Q_{tot}} = \frac{1}{1 + \exp\left[\frac{-z_k F(V - V_q)}{RT}\right]} \tag{A7}$$

Rearrangement of Eq. A6 gives an explicit expression for the midpoint voltage V_q:

$$V_q = \frac{RT}{\delta F} \ln\left[\frac{k_{-1}(0)[Na]_0}{k_1}\right] \tag{A8}$$

For a two-state model V_q is also equal to V_k, the voltage at which $k_1 = k_{-1}$. Thus, for a univalent charged species, the change in the midpoint of the Q vs. V relationship expected for a change of $[Na]_0$ from $[Na]_1$ to $[Na]_2$ is

$$\Delta V_q = \frac{RT}{\delta F} \ln\left(\frac{[Na]_2}{[Na]_1}\right) \tag{A9}$$

A similar derivation of the shift of the midpoint of the Na/Na exchange-mediated efflux vs. voltage relationship was originally obtained by Gadsby, De Weer, and Rakowski (manuscript submitted for publication), who suggested the application of the equation to I-V relationships and to pre–steady-state charge movement.

Pseudo Three-State Model of Na Translocation

Consider the pseudo three-state reaction scheme (Fig. 10 B), in which k_1, k_{-1}, k_2, and $k_{-2}(0)$ are voltage-independent rate constants and k_{-2} is a voltage-dependent, pseudo first-order rate coefficient. The equation for the rate coefficient k_{-2} can be derived in the same way as Eq. A2:

$$k_{-2} = k_{-2}(0)[Na]_0^n \exp\left(-z_k FV/RT\right) \tag{A10}$$

We define

$$E_{tot} = E_i + E_{Na} + E_0 \tag{A11}$$

and obtain the following differential equation for this reaction scheme:

$$\frac{d^2 E_0}{dt^2} + C_1 \frac{dE_0}{dt} + C_2 E_0 = C_3 E_{tot} \tag{A12}$$

Where

$$C_1 = k_1 + k_{-1} + k_2 + k_{-2} \tag{A13}$$

$$C_2 = k_1 k_2 + k_1 k_{-2} + k_{-1} k_{-2} \tag{A14}$$

$$C_3 = k_1 k_2 \tag{A15}$$

Eq. A12 may be solved for the initial conditions $E_0(0) = 0$ and $dE_0(0)/dt = 0$ to give

$$E_0(t) = C_3 E_{tot} \left[\frac{1}{ab} + \frac{be^{-at} - ae^{-bt}}{ab(a - b)} \right] \tag{A16}$$

where

$$a = \frac{C_1 + \sqrt{C_1^2 - 4C_2}}{2} \tag{A17}$$

and

$$b = \frac{C_1 - \sqrt{C_1^2 - 4C_2}}{2} \tag{A18}$$

Steady-State Charge Distribution for the Pseudo Three-State Model

Since $ab = C_2$ and $Q(t)$ is proportional to $E_0(t)$, the steady-state solution of Eq. A16 may be written as

$$\frac{Q(V, \infty)}{Q_{tot}} = \frac{C_3}{C_2} = \frac{1}{1 + \left[\dfrac{1}{k_2} + \dfrac{k_{-1}}{k_1 k_2} \right] k_{-2}} \tag{A19}$$

Substituting Eq. A10 in Eq. A19 and defining a midpoint voltage V_q such that

$$\left[\frac{k_{-2}(0)}{k_2} + \frac{k_{-2}(0)k_{-1}}{k_1 k_2} \right] [Na]_0^n = \exp \left[\frac{z_k F V_q}{RT} \right] \tag{A20}$$

we obtain

$$\frac{Q(V, \infty)}{Q_{tot}} = \frac{1}{1 + \exp \left[\dfrac{-z_k F(V - V_q)}{RT} \right]} \tag{A21}$$

which is identical to the steady-state charge distribution function for the pseudo two-state model (Eq. A7) except for the definition of V_q.

We may rearrange Eq. A20 to obtain an explicit expression for V_q for the pseudo three-state model:

$$V_q = \frac{RT}{\delta F} \ln \left[\frac{(k_1 + k_{-1})k_{-2}(0)[Na]_0}{k_1 k_2} \right] \tag{A22}$$

The change in midpoint voltage V_q expected for a change in $[Na]_0$ for the pseudo three-state model is, therefore, also given by Eq. A9 previously derived for the pseudo two-state model. The general conclusion may be drawn that addition of voltage-independent transitions to the left of the final voltage-dependent step in the reaction scheme may affect the absolute value of the midpoint voltage V_q, but will not change the ΔV_q expected for a change in external [Na].

Voltage Dependence of the Pre–Steady-State Current Relaxation Rate Coefficient for the Pseudo Three-State Model

The time course of the current transient may be obtained by differentiation of Eq. A16:

$$I(t) = \frac{1}{a - b} (e^{-bt} - e^{-at}) \tag{A23}$$

This indicates that, in general, the transient current will have a rising phase as well as a falling

phase. Since a and b are solutions of a quadratic equation, however, the behavior of this function is not immediately apparent. Further insight, however, can be gained by considering the special case $4C_2/C_1^2 \ll 1$. Following Simon (1972; p. 78) we may approximate $\sqrt{C_1^2 - 4C_2}$ by $C_1 - (2C_2/C_1)$. In this case

$$a = C_1 - \frac{C_2}{C_1} \tag{A24}$$

and

$$b = C_2/C_1 \tag{A25}$$

Substituting Eqs. A24 and A25 in Eq. A23 gives

$$\frac{dE_0(t)}{dt} = \frac{C_1}{C_1^2 - 2C_2}\left\{\exp\left(\frac{-C_2 t}{C_1}\right) - \exp\left[-\left(C_1 - \frac{C_2}{C_1}\right)t\right]\right\} \tag{A26}$$

Eq. A26 predicts a transient current with a rising and falling phase in which the relaxation rate of the falling phase, k_{tot}, is C_2/C_1 or

$$k_{tot} = \frac{k_1 k_2 + (k_1 + k_{-1})k_{-2}}{k_1 + k_{-1} + k_2 + k_{-2}} \tag{A27}$$

This expression for k_{tot} may be divided into two terms and V_k defined as the voltage at which these two terms are equal:

$$k_1 k_2 = (k_1 + k_{-1})k_{-2} \tag{A28}$$

Substituting Eq. A10 in Eq. A28 for $V = V_k$ and solving for V_k gives

$$V_k = \frac{RT}{\delta F}\ln\left[\frac{(k_1 + k_{-1})k_{-2}(0)[\text{Na}]_0}{k_1 k_2}\right] \tag{A29}$$

which is identical in form to Eq. A22, thus demonstrating that for this simplification of the pseudo three-state model $V_k = V_q$, as it must since V_k represents the voltage at which the forward and backward rates associated with E_0 are equal. We may write expressions for the forward (k_f) and backward (k_b) rates by separating Eq. A27 into two terms and rearranging:

$$k_f = \frac{\dfrac{k_1 k_2}{(k_1 + k_{-1} + k_2)}}{1 + \dfrac{k_{-2}}{(k_1 + k_{-1} + k_2)}} \tag{A30}$$

$$k_b = \frac{k_1 + k_{-1}}{1 + \dfrac{(k_1 + k_{-1} + k_2)}{k_{-2}}} \tag{A31}$$

Eq. A10 may be substituted in Eqs. A30 and A31 to give after rearrangement

$$k_f = \frac{\dfrac{k_1 k_2}{(k_1 + k_{-1} + k_2)}}{1 + \dfrac{k_{-2}(0)[\text{Na}]_0^n}{(k_1 + k_{-1} + k_2)}\exp\left[\dfrac{-z_k FV}{RT}\right]} \tag{A32}$$

$$k_b = \frac{k_1 + k_1}{1 + \dfrac{(k_1 + k_{-1} + k_2)}{k_{-2}(0)[\text{Na}]_0^n}\exp\left[\dfrac{z_k FV}{RT}\right]} \tag{A33}$$

We may define a midpoint voltage for the sigmoid curve describing the forward and backward rates, V_{fb}, such that

$$\frac{k_{-2}(0)[Na]_0^n}{(k_1 + k_{-1} + k_2)} = \exp\left[\frac{z_k F V_{fb}}{RT}\right] \tag{A34}$$

Substituting Eq. A34 into Eqs. A32 and A33 we obtain

$$k_f = \frac{\dfrac{k_1 k_2}{k_1 + k_{-1} + k_2}}{1 + \exp\left[\dfrac{-z_k F(V - V_{fb})}{RT}\right]} \tag{A35}$$

$$k_b = \frac{k_1 + k_{-1}}{1 + \exp\left[\dfrac{z_k F(V - V_{fb})}{RT}\right]} \tag{A36}$$

Eqs. A35 and A36 show that the forward and backward rates of current relaxation for the pseudo three-state model are sigmoid functions of voltage having the same midpoint voltage, V_{fb}. We may write an explicit expression for V_{fb} from Eq. A34.

$$V_{fb} = \frac{RT}{\delta F} \ln\left[\frac{k_{-2}(0)[Na]_0}{k_1 + k_{-1} + k_2}\right] \tag{A37}$$

Note that the midpoint voltage of the sigmoid distribution of k_f and k_b described by Eq. A37 is not identical to the midpoint voltage of the Q vs. V distribution (Eq. A22) at which k_f equals k_b. This can occur since the maximum forward and backward rates measured at infinite positive or negative voltages (the terms in the numerator of Eqs. A35 and A36, respectively) are not necessarily equal.

REFERENCES

Abercrombie, R. F., and P. De Weer. 1978. Electric current generated by squid giant axon sodium pump: external K and internal ADP effects. *American Journal of Physiology.* 235:C63–C68.

Bahinski, A., M. Nakao, and D. C. Gadsby. 1988. Potassium translocation by the Na/K pump is voltage insensitive. *Proceedings of the National Academy of Sciences, USA.* 85:3412–3416.

Borlinghaus, R., H.-J. Apell, and P. Läuger. 1987. Fast charge translocations associated with partial reactions of the Na,K pump. I. Current and voltage transients after photochemical release of caged ATP. *Journal of Membrane Biology.* 97:161–178.

Chandler, W. K., R. F. Rakowski, and M. F. Schneider. 1976. A noninear voltage-dependent charge movement in skeletal muscle. *Journal of Physiology.* 254:245–284.

Cornelius, F. 1989. Uncoupled Na⁺-efflux on reconstituted shark rectal gland Na,K-ATPase is electrogenic. *Biochemical and Biophysical Research Communications.* 160:801–807.

De Weer, P. 1990. The Na/K pump: a current generating enzyme. *In* Regulation of Potassium Transport across Biological Membranes. L. Reuss, G. Szabo, and J. M. Russell, editors. University of Texas Press, Austin, TX. 5–22.

De Weer, P., D. C. Gadsby, and R. F. Rakowski. 1993. An external access channel determines the voltage sensitivity of both Na/Na exchanging and backward-running modes of the sodium pump. *Biophysical Journal.* (Abstr.) In press.

De Weer, P., R. F. Rakowski, and D. C. Gadsby. 1992. Kinetic evidence that the Na/K pump delivers Na^+ to the cell exterior through a high-field channel. *Biophysical Journal.* 61:A135. (Abstr.)

Fendler, K., E. Grell, M. Haubs, and E. Bamberg. 1985. Pump currents generated by the purified Na^+,K^+-ATPase from kidney on black lipid membranes. *EMBO Journal.* 4:3079–3085.

Garrahan, P. J., and I. M. Glynn. 1967a. The behavior of the sodium pump in red cells in the absence of external potassium. *Journal of Physiology.* 192:159–174.

Garrahan, P. J., and I. M. Glynn. 1967b. Factors affecting the relative magnitudes of the sodium: potassium and sodium:sodium exchanges catalyzed by the sodium pump. *Journal of Physiology.* 192:189–216.

Garrahan, P. J., and I. M. Glynn. 1967c. The incorporation of inorganic phosphate into adenosine triphosphate by reversal of the sodium pump. *Journal of Physiology.* 192:237–257.

Glynn, I. M. 1984. The electrogenic sodium pump. *In* Electrogenic Transport: Fundamental Principles and Physiological Implications. M. P. Blaustein and M. Lieberman, editors. Raven Press, New York. 33–48.

Hilgemann, D. W., K. D. Philipson, and D. A. Nicoll. 1992. Possible charge movement of extracellular Na^+ binding by Na/K pump and cardiac Na/Ca exchanger in giant patches. *Biophysical Journal.* 61:A390. (Abstr.)

Holmgren, M., and R. F. Rakowski. 1993. Equality of on and off charge movement by the Na/K pump in *Xenopus* oocytes. *Biophysical Journal.* (Abstr.) In press.

Lagnado, L., L. Cervetto, and P. A. McNaughton. 1988. Ion transport by the Na-Ca exchange in isolated rod outer segments. *Proceedings of the National Academy of Sciences, USA.* 85:4548–4552.

LaTona, J. 1990. Ion concentration and voltage dependence of Na/K pump current in *Xenopus laevis* oocytes. Ph.D. thesis. The University of Health Sciences/The Chicago Medical School, North Chicago, II. University Microfilms, Ann Arbor, MI. 1–84.

Läuger, P. 1991. Electrogenic Ion Pumps. Sinauer Associates, Inc., Sunderland, MA. 212–219.

Läuger, P., and H.-J. Apell. 1988. Transient behavior of the Na^+/K^+ pump: microscopic analysis of nonstationary ion-translocation. *Biochimica et Biophysica Acta.* 944:451–464.

Lee, K. H., and R. Blostein. 1980. Red cell sodium fluxes catalyzed by the sodium pump in the absence of K^+ and ADP. *Nature.* 285:338–339.

Mitchell, P., and J. Moyle. 1974. The mechanism of proton translocation in reversible proton-translocating adenosine triphosphatases. *Biochemical Society (Special Publication).* 4:91–111.

Nagel, G. A., M. Suenson, M. Nakao, and D. C. Gadsby. 1991. Transient and stationary Na/K pump currents in guinea pig ventricular myocytes at external sodium concentrations up to 250 mM. *Biophysical Journal.* 59:340a. (Abstr.)

Nakao, M., and D. C. Gadsby. 1986. Voltage dependence of Na translocation by the Na/K pump. *Nature.* 323:628–630.

Polvani, C., and R. Blostein. 1988. Protons as substitutes for sodium and potassium in the sodium pump reaction. *Journal of Biological Chemistry.* 264:16757–16763.

Rakowski, R. F. 1992. Presteady-state charge movement by the Na/K pump. *Biophysical Journal.* 61:A135. (Abstr.)

Rakowski, R. F., L. A. Vasilets, J. LaTona, and W. Schwarz. 1991. A negative slope in the current-voltage relationship of the Na^+/K^+ pump in *Xenopus* oocytes produced by reduction of external $[K^+]$. *Journal of Membrane Biology.* 121:177–187.

Sagar, A., V. Wallner, and R. F. Rakowski. 1993. Current-voltage relationships of the Na/K pump in *Xenopus* ooxytes analyzed using an access channel model. *Biophysical Journal.* (Abstr.) In press.

Simon, W. 1972. Mathematical Techniques for Biology and Medicine. MIT Press, Cambridge, MA. 291 pp.

Taglialatela, M., L. Toro, and E. Stefani. 1992. Novel voltage clamp to record small, fast currents from ion channels expressed in *Xenopus* oocytes. *Biophysical Journal.* 61:78–82.

Vasilets, L., H. S. Omay, T. Ohata, S. Noguchi, M. Kawamura, and W. Schwarz. 1991. Stimulation of the Na^+/K^+ pump by external $[K^+]$ is regulated by voltage-dependent gating. *Journal of Biological Chemistry.* 266:16285–16288.